

MIT Open Access Articles

One-step generation of monoclonal B cell receptor mice capable of isotype switching and somatic hypermutation

The MIT Faculty has made this article openly available. **Please share** how this access benefits you. Your story matters.

Citation: Jacobsen, Johanne T. et al. "One-step generation of monoclonal B cell receptor mice capable of isotype switching and somatic hypermutation." *Journal of Experimental Medicine* 215, 10 (September 2018): 2686–2695 © 2018 Jacobsen et al

As Published: <http://dx.doi.org/10.1084/jem.20172064>

Publisher: Rockefeller University Press

Persistent URL: <https://hdl.handle.net/1721.1/125966>

Version: Final published version: final published article, as it appeared in a journal, conference proceedings, or other formally published context

Terms of use: Creative Commons Attribution-Noncommercial-Share Alike



TECHNICAL ADVANCES

One-step generation of monoclonal B cell receptor mice capable of isotype switching and somatic hypermutation

Johanne T. Jacobsen^{1,2}, Luka Mesin¹, Styliani Markoulaki³, Ariën Schiepers¹, Cecília B. Cavazzoni^{1,4}, Djenet Bousbaine⁵, Rudolf Jaenisch³, and Gabriel D. Vitoria¹

We developed a method for rapid generation of B cell receptor (BCR) monoclonal mice expressing prerrearranged *Igh* and *Igk* chains monoallelically from the *Igh* locus by CRISPR-Cas9 injection into fertilized oocytes. B cells from these mice undergo somatic hypermutation (SHM), class switch recombination (CSR), and affinity-based selection in germinal centers. This method combines the practicality of BCR transgenes with the ability to study Ig SHM, CSR, and affinity maturation.

Introduction

Genetically modified mice expressing predefined monoclonal B cell receptor (BCR) repertoires are essential tools in immunological research. The first monoclonal BCR mice were generated by injection of plasmids encoding heavy and light Ig chains that integrated together at random sites in the genome (Mason et al., 1992). These mice have greatly advanced our understanding of aspects of immune regulation such as allelic exclusion of antibody V region genes (Rusconi and Köhler, 1985; Weaver et al., 1985; Nussenzweig et al., 1987; Manz et al., 1988) and B cell tolerance to neo-self-antigens (Goodnow et al., 1988, 1989) or true self-antigens (Ewulonu et al., 1990; Bloom et al., 1993; Benschop et al., 2001). Although mice can be generated relatively rapidly using this strategy, the fact that the transgenic BCR is expressed from a nonnative locus leads to important shortcomings. First, because downstream isotypes are usually not incorporated into the transgenes, B cells from these mice cannot perform class switch recombination (CSR). Furthermore, since transgenes frequently integrate into the genome in multiple copies, mice with transgenic BCRs cannot undergo monoallelic somatic hypermutation (SHM), a prerequisite for proper affinity maturation. Thus, classic BCR transgenic mice are inadequate models for some of the key phenomena in B cell immunology. To circumvent these issues, a second generation of mice was created in which prerassembled V_H and/or V_L regions are inserted into their native loci by homologous recombination (Taki et al., 1993; Pelanda et al., 1996). These mice are capable of SHM and CSR and thus allow a wider range of phenomena to be studied. However, traditional knock-in technology relies on labor-intensive genetic

editing of embryonic stem cells, and two separate mouse strains must be targeted, one for the Ig heavy chain (IgH) and one for the Igλ/κ light chain. This double-knock-in approach also requires more complex breeding strategies in order to maintain both Ig chains together after initial generation or upon crossing to other targeted alleles.

Recently, the CRISPR-Cas9 programmable nuclease has been shown to efficiently induce double-stranded breaks in DNA in fertilized oocytes (Yang et al., 2013), enabling homology-directed incorporation of transgenes directly at this stage. We took advantage of this technology to target a bicistronic allele encoding both the light and the heavy Ig chains to the endogenous *Igh* locus. Thus, in a single step, we were able to generate monoallelic BCR monoclonal mice capable of CSR, SHM, and affinity maturation in the same time frame required for untargeted BCR transgenics.

Results

We began by determining which single-guide RNAs (sgRNAs) were optimal for generating double-stranded breaks at the 5' and 3' ends of an ~2.3-Kbp region spanning the four J segments of the *Igh* locus (Fig. 1, a and b). Cutting efficiency was assayed for several sgRNAs by cytoplasmic injection of in vitro transcribed sgRNA and Cas9 mRNA into fertilized oocytes, as previously described (Sakurai et al., 2014). Cutting was determined by extracting DNA from single blastocysts at embryonic day 4.5 (E4.5), amplifying the region around the Cas9 targeting site by PCR, and Sanger sequencing the PCR product. In case of

¹Laboratory of Lymphocyte Dynamics, The Rockefeller University, New York, NY; ²Center for Immune Regulation, Oslo University Hospital, University of Oslo, Oslo, Norway; ³Whitehead Institute for Biomedical Research, Cambridge, MA; ⁴Carlos Chagas Filho Biophysics Institute, Federal University of Rio de Janeiro, Rio de Janeiro, Brazil; ⁵Boston Children's Hospital, Harvard Medical School, Boston, MA.

Correspondence to Gabriel D. Vitoria: vitoria@rockefeller.edu; Johanne T. Jacobsen: jjacobsen@rockefeller.edu.

© 2018 Jacobsen et al. This article is distributed under the terms of an Attribution–Noncommercial–Share Alike–No Mirror Sites license for the first six months after the publication date (see <http://www.rupress.org/terms/>). After six months it is available under a Creative Commons License (Attribution–Noncommercial–Share Alike 4.0 International license, as described at <https://creativecommons.org/licenses/by-nc-sa/4.0/>).

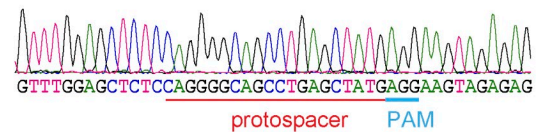
successful Cas9-mediated cleavage, insertions/deletions in one or both alleles are discernible as an altered pattern of chromatogram peaks (Fig. 1 a). We defined as efficient any sgRNAs that cut at least 50% of blastocysts analyzed. Our final 5' and 3' sgRNAs cut 15/21 and 3/5 blastocysts, respectively (Fig. 1 b). The cut site for our final 5' sgRNA (ID 6) was located 633 bp upstream of J_H1 , and the cut site for our 3' sgRNA (ID 7) was located 108 bp downstream of J_H4 .

To build a monoallelic light/heavy chain Ig construct, we chose an unmutated B cell clone specific for the model antigen chicken gamma globulin (CGG; more specifically, the clone recognizes the constant region of IgY, the major component of CGG) that was efficiently recruited to germinal centers (GCs) upon CGG immunization in a polyclonal setting (Tas et al., 2016). The targeting construct for the *Igh*^{CGG} allele consisted of a commonly used Ig V-region promoter (Dosenovic et al., 2015; Escolano et al., 2016) followed by a prerrearranged Igκ VJ segment, a human Igκ constant region (human Igκ; Casellas et al., 2001) was used for subsequent identification of cells bearing the transgenic receptor), a self-cleaving porcine teschovirus 2A (P2A) peptide, and a prerrearranged IgH VDJ segment (Fig. 2 a). When targeted to the *Igh* J locus, this construct configuration results in the expression of both light and heavy chain proteins from the same promoter, with the heavy chain variable region spliced onto the endogenous IgH constant region. The 2A peptide sequence allows for stoichiometric expression of the light and heavy Ig chains. To reduce focused activation-induced cytidine deaminase (AID) targeting in the region encoding human Igκ and 2A peptide, we eliminated all AID hotspot motifs (RGYW) from this sequence by introduction of silent mutations (Fig. S1). This construct was cloned into a targeting vector containing 5' and 3' homology arms of 7.9 and 3.4 kb, respectively, which was previously used for generating *Igh* targeted insertions in C57BL/6 embryonic stem cells (Dosenovic et al., 2015). As with the sgRNAs, the homology arms flank the endogenous J segments, removing this section of the *Igh* locus upon successful homology-directed repair and thus preventing further rearrangement of the targeted locus.

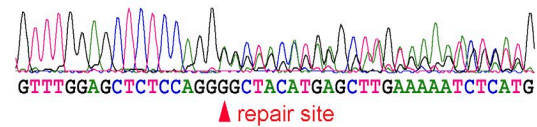
To determine whether the P2A peptide, which remains attached to the C terminus of the Igκ chain, affects antibody functionality, we produced the full anti-CGG mAb (Tas et al., 2016) recombinantly, with or without addition of the P2A cleavage product to the C terminus of Cκ. Binding of the two recombinant mAbs to chicken IgY was indistinguishable (Fig. 2 b), indicating that bicistronic expression using a P2A peptide does not affect the binding properties of the resulting antibody.

Cytoplasmic zygote injection of the bicistronic targeting construct (Fig. 2 a) along with Cas9 mRNA, sgRNAs 6 and 7 (Fig. 1 b), and an inhibitor of nonhomologous end joining (Maruyama et al., 2015) yielded 1 out of 12 and 1 out of 11 pups positive for human Igκ in two independent experiments. These F₀ mice displayed a relatively low proportion of B cells carrying the engineered receptor (Fig. 2 c), indicative of mosaicism resulting from targeting taking place after the first chromosome duplication. Upon breeding, human Igκ⁺ mice (*Igh*^{CGG/+}) were born at sub-Mendelian ratios, and positive F₁ mice carried a high proportion of B cells expressing the engineered receptor (Fig. 2 d), supporting the notion of mosaic targeting of the F₀ mouse. We validated the

a WT allele



Heterozygous cut/repair



b

Id	guide sequence	strain	site	cut
1	gagtcctgtgtctctgac	C57Bl/6	5'	1/17
2	actgttttgagagaaatcat	C57Bl/6	5'	1/19
3	tgtgtgtctctgactggtgca	C57Bl/6	5'	0/18
4	ggagcaccacagtgttaact	C57Bl/6	5'	0/10
5	tgagctatgaggaagtagag	C57Bl/6	5'	3/11
6	caggggcagcctgagctatg	C57Bl/6	5'	15/21
7	ggagccggctgagagaagt	C57Bl/6	3'	3/5
8	catactctgtgctagtgtg	BDF1/B6	5'	3/13
1	gagtcctgtgtctctgac	BDF1/B6	5'	3/15
1	gagtcctgtgtctctgac	BDF1	5'	5/6

Figure 1. Efficiency of sgRNAs flanking the mouse J_H region. (a) Example chromatograms obtained by blastocyst PCR, 4 d after CRISPR-Cas9-mediated targeting by zygote injection. WT (protospacer and PAM indicated; top) and successfully targeted blastocysts (bottom). Note the altered peaks resulting from a monoallelic indel at the position indicated with an arrowhead (repair site). (b) List of tested sgRNA protospacer sequences, including mouse strain, location (5' or 3' of the J segments), and efficiency of cutting measured as in panel a. The final sgRNAs used for generating knock-in mice are in bold font.

integration of our construct into the *Igh* locus by Southern blotting of a heterozygous F₁ mouse (Fig. 2 d).

To determine whether presence of the *Igh*^{CGG} allele affected peripheral B cell populations, we analyzed the spleen of *Igh*^{CGG/+} mice for follicular (Fo; CD93⁺ CD23⁺ CD21^{lo} IgM⁺), marginal zone (MZ; CD93⁺ CD23⁺ CD21^{hi} IgM^{hi}), and B1 (CD93⁺ CD23⁺ CD21^{int} IgM^{int}) B cells, as previously described (Sweet et al., 2010). CGG-binding *Igh*^{CGG/+} B cells showed normal B cell subset distribution when compared with WT mice, with the exception of a slight skewing of human Igκ⁺ CGG-binding cells away from the MZ (and hence toward the Fo) subset when compared with B cells from the same mouse that did not express the transgene (Fig. 3, a and b). Similar results were obtained for skin-draining LNs (Fig. 3 b). Peritoneal B1 cells were largely absent from the CGG-binding fraction of *Igh*^{CGG/+} mice (Fig. 3 c), in line with the notion that the B1 lineage is largely determined by BCR specificity (Lam and Rajewsky, 1999).

B cells expressing the prerrearranged receptor showed almost complete allelic exclusion of the endogenous mouse heavy chain (Fig. 4 a), as shown by crossing the *Igh*^{CGG} allele (which is linked to the C57BL/6 *Igh* "b" allotype) onto a congenic C57BL/6 *Igh*^a background. Similar exclusion was seen for the endogenous (mouse) Igκ and Igλ chains (Fig. 4 a). Mature follicular CGG-binding B cells showed lower mean expression of surface IgM and IgD when compared with WT polyclonal cells, although expression of both isotypes was still within the range observed in polyclonal B

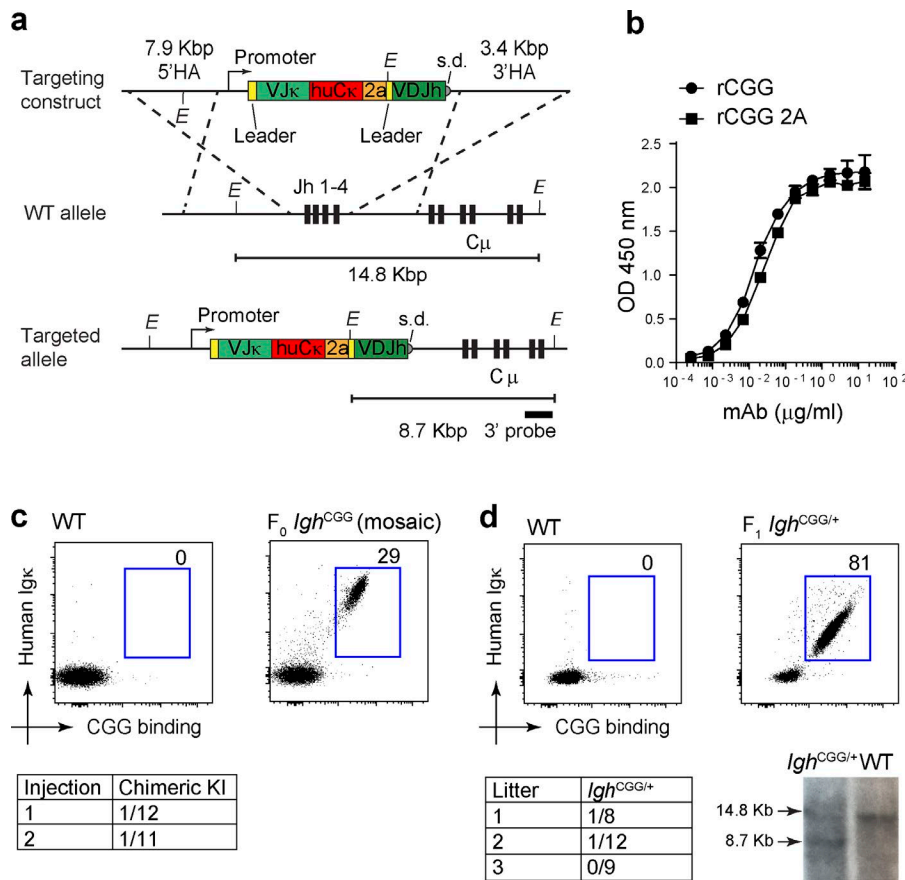


Figure 2. Generation of a bicistronic VJcκ-VDJh CGG-specific knock-in mouse. (a) Schematic representation of the bicistronic VJcκ-2A-VDJh targeting cassette used to generate the *Igh*^{CGG} allele, before and after targeting to the *Igh* locus. The total insert size is 1.7 Kbp. The 3' probe used for Southern blot is indicated. s.d., splice donor; E, EcoRV. Segments are not drawn to scale. (b) ELISA showing binding to IgY of recombinant WT anti-CGG mAb (rCGG) and recombinant anti-CGG mAb with the 2A cleavage product attached to the Cκ C terminus (rCGG 2A). Error bars are SD of technical replicates. (c) Flow cytometry of blood samples, gated on B220⁺ cells, showing expression of human Igκ and CGG binding. One WT and one correctly targeted founder mouse are shown. Frequency of *Igh*^{CGG}-positive founders in two rounds of injection is shown below (positive/total pups). Numbers within flow plots indicate percentage of cells in the designated gate. (d) Germline transmission of *Igh*^{CGG} to F₁ mice. One *Igh*^{CGG} founder female was mated to a C57BL/6 male, and positive offspring in sequential litters were determined by flow cytometry as in panel c. Frequency of *Igh*^{CGG/+} F₁ pups (positive/total) in each litter is shown below. A Southern blot confirming integration into the *Igh* locus is also shown. An intact germline *Igh* locus yields a 14.8-kb fragment, while integration into the locus yields a 8.7-kb fragment.

cells (Fig. 4 b). Lower surface Ig (sIg) expression was not due to overt failure of the 2A peptide to induce ribosome skipping and subsequent separation of light and heavy chains, since the full length VJcκ-VDJcμ protein (~95-kD band) could not be detected by anti-IgM Western blot of naive *Igh*^{CGG/+} B cells (Fig. 4 c). While the reasons for lower sIg expression in these mice are unclear, sIg levels in B cells are potentially a clonal property, in that different monoclonal B cell mice display different levels of sIg (Goodnow et al., 1988; Chen et al., 2013). Therefore, we cannot determine whether the low sIg expression seen in *Igh*^{CGG/+} mice is a consequence of our knock-in strategy or of the specific CGG-reactive clone we used to generate this strain.

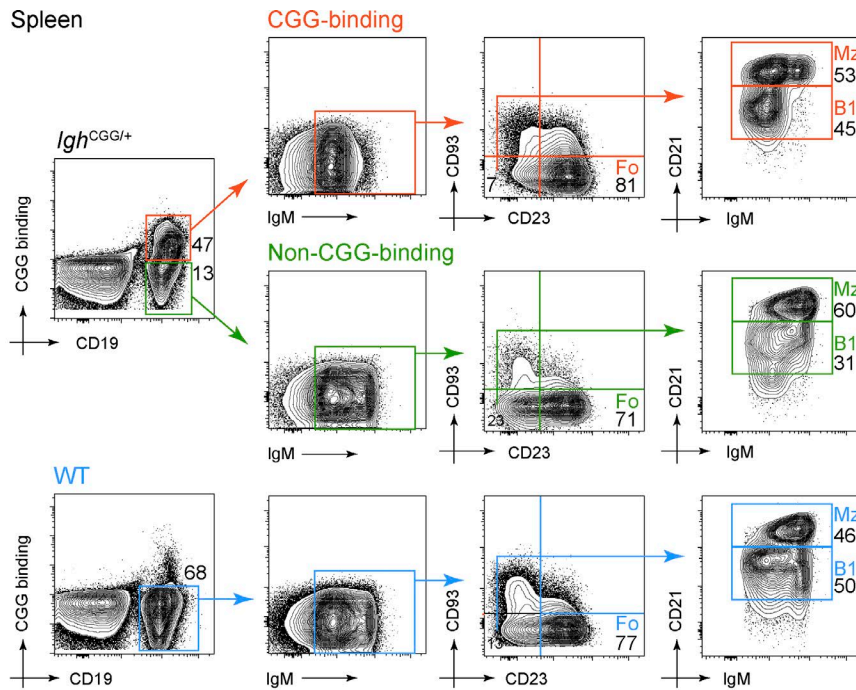
We next sought to determine whether *Igh*^{CGG/+} B cells were fully functional in spite of their lower expression of sIg. We first cultured splenic B cells in vitro with LPS and IL-4 to induce isotype switching to IgG₁. *Igh*^{CGG/+} B cells switched to IgG₁ at WT levels, although surface expression of this isotype was again slightly lower than WT (Fig. 5 a). To determine the ability of *Igh*^{CGG/+} B cells to differentiate into plasmablasts and secrete Ig in vitro, we cultured sorted WT or CGG-binding *Igh*^{CGG/+} B2 follicular B cells (sorted as in Fig. 3 a) for 4 d in LPS and IL-4. Plasmablast differentiation (detected as the percentage of cells that up-regulated CD138/Syndecan-1) and secretion of IgG₁ into the supernatant were comparable between WT and monoclonal B cells (Fig. 5 b).

To determine their ability to respond to antigen in vivo, we adoptively transferred *Igh*^{CGG/+} B cells into a CD45.1 congenic strain, which we immunized with CGG precipitated in alum. *Igh*^{CGG/+} B cells were able to access GCs and class switch to IgG₁,

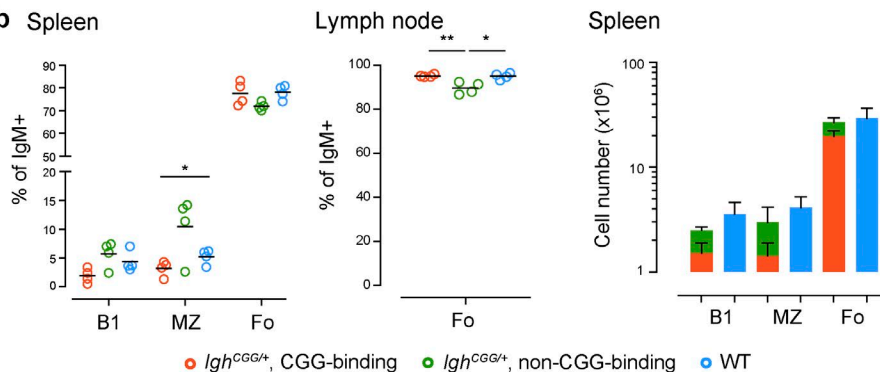
indicating that these cells are capable of proper progression through all steps of B cell activation. Recipient mice also developed readily detectable titers of IgY-binding human Igκ, indicative of plasmablast/plasma cell differentiation (Fig. 6 b). Western blotting of serum for human Igκ under nonreducing and reducing conditions showed single bands of 150–250 kD and ~25–30 kD in size, respectively, indicating proper disulfide bonding of heavy and light chains in the presence of the P2A cleavage product immediately downstream of the C-terminal cysteine residue of Igκ. Thus, despite their lower expression of sIg, *Igh*^{CGG/+} cells are competent to engage in GC reactions, undergo CSR, and differentiate into antibody-secreting cells in vivo.

To assess the ability of *Igh*^{CGG/+} B cells to undergo SHM and affinity maturation, we analyzed the mutation patterns of single GC B cells sorted from experiments analogous to those detailed in Fig. 5 b. *Igh*^{CGG/+} B cells accumulated substantial SHM across the entire engineered locus (Fig. 4, c–e). Removal of AID hotspots from human *Igk* and 2A peptide led to a slight reduction in SHM in these regions (Fig. 5, c and e), compatible with the partial requirement for the “hotspot” motif in AID targeting (Yu et al., 2004). The accumulation of mutations at similar positions (tall peaks in Fig. 5 c) in VJcκ and VDJh, but not in Cκ or 2A, suggested that antigen-based selection was active on this allele. To verify this, and to determine whether SHM burdens in *Igh*^{CGG/+} B cells were comparable to those of WT B cells, we took advantage of the fact that we had previously characterized the SHM and evolution of this particular anti-CGG clone in two separate GCs in vivo (Tas et al., 2016). We therefore have

a Spleen



b Spleen



c Peritoneum

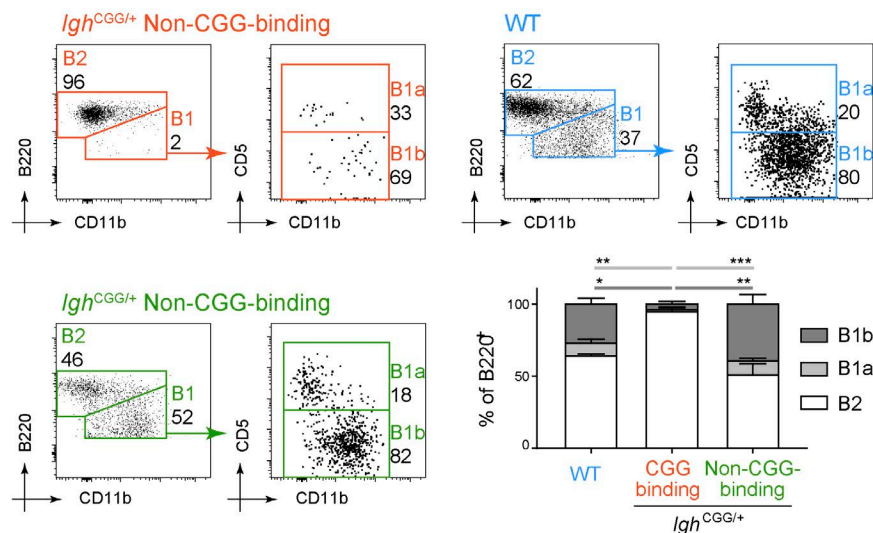


Figure 3. B cell subsets and sIg expression in *Igh*^{CGG/+} mice. (a) Splenocytes from 6-wk-old *Igh*^{CGG/+} or WT C57BL/6 mice were stained as indicated. For *Igh*^{CGG/+} mice, CD19⁺ cells were analyzed separately as either CGG binding or nonbinding, the latter representing B cells that escaped the transgene. B cells were classified as Fo (CD93⁻ CD23⁺ CD21^{lo} IgM⁺), MZ (CD93⁻ CD23⁻ CD21^{hi} IgM^{hi}), and B1 (CD93⁻ CD23⁻ CD21^{int} IgM^{int}). WT mice were analyzed identically on the total CD19⁺ population. Error bars are SD of biological replicates. (b) Summary of splenic data as in panel a for four mice of each genotype. MZ, B1, and Fo B cells are shown as percentage of all IgM⁺ cells for WT mice or as percentage of IgM⁺ cells of that class (CGG binding or nonbinding) *Igh*^{CGG/+} mice. *, *P* = 0.039 (unpaired *t* test). Fo B cells were also analyzed in skin-draining LNs (center), and splenic B cell subsets are also shown as absolute numbers (right). (c) B1b, B1a, and B2 B cell subset distribution in the peritoneal cavity of *Igh*^{CGG/+} and WT mice. Representative dot plots of B2 (B220⁺ CD11b⁻), B1a (B220⁺ CD11b⁺ CD5⁺) and B1b (B220⁺ CD11b⁺ CD5⁻) from the CGG-binding and nonbinding population of *Igh*^{CGG/+} and WT mice. Bar graphs show summarized subset distribution of the B2, B1a, and B1b B cells from *n* = 3 *Igh*^{CGG/+} and *n* = 2 WT mice from two independent experiments. *, *P* ≤ 0.05; **, *P* ≤ 0.01; ***, *P* ≤ 0.001 (unpaired *t* test). Numbers within flow plots indicate percentage of cells in the designated gate.

a previous record of the maturation of this very clone under WT conditions, with which we could compare the evolution of our transgenic B cells. To avoid unfair comparisons imposed by the presence of a strong selective bottleneck, we chose a GC in

which this clone was expanded in several parallel sublineages rather than by a single selective sweep (see Fig. 4, "LN#2 GC#2," in Tas et al., 2016). We then compared the SHM pattern of cells from this GC to that of *Igh*^{CGG/+} GC B cells pooled from two whole

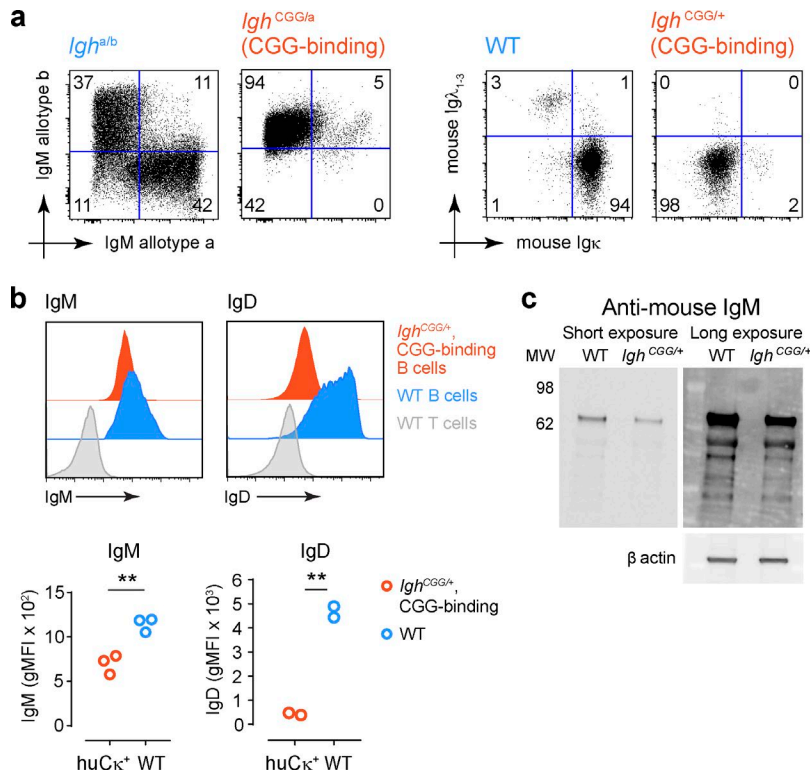


Figure 4. BCR expression in *IgH^{CGG}* mice. (a) Left: Flow cytometry of splenic B cells (B220-gated) from *IgH^{CGG/a}* mice (where the *IgH^{CGG}* allele carries the IgM^b allotype and the WT allele carries the IgM^a allotype) compared with *IgH^{a/b}* mice (where both IgM^a and IgM^b alleles are WT). Right: Flow cytometry of splenic B cells from *IgH^{CGG/+}* and WT mice showing allelic exclusion of endogenous Cκ and Cλ chains. One plot representative of three mice is shown for each. Numbers within flow plots indicate percentage of cells in the quadrant. (b) SIgM and IgD expression on WT and *IgH^{CGG/+}* follicular B cells. Gated on CD19⁺/human Cκ⁺/CD93⁻/CD23⁺ cells for *IgH^{CGG/+}* mice or on CD19⁺/CD93⁻/CD23⁺ cells for WT. WT T cells are shown as a negative control. Data from independent experiments are shown on the right. Each symbol represents one mouse. **, P < 0.01 (unpaired t test). gMFI, geometric mean fluorescence intensity. (c) Western blot for IgM in naive B cells from *IgH^{CGG/+}* mice. Anti-IgM signal for WT and anti-*IgH^{CGG/+}* B cells is shown at two different exposures. The relevant band is indicated at ~70 kD. The β actin loading control is shown below. Note the absence of an ~95-kb band, the expected size of the uncleaved Vκ/V_H construct. Data are representative of two experiments.

LN. This analysis showed that SHM in *IgH^{CGG/+}* B cells reached a substantial fraction of the levels seen in this particular GC at the same time point (49% for *Igk* VJ and 61% for *IgH* VDJ; Fig. 5 e). More importantly, comparison of WT and *IgH^{CGG/+}* B cells showed a remarkable coincidence in the most frequently mutated positions (red bars in Fig. 5 f), including accumulation of an Igκ mutation (C119>G) showed to confer an eightfold increase in affinity to this clone and that was strongly selected in WT GCs (Tas et al., 2016). By reconstructing phylogenetic trees of VJκ, we could identify three separate clusters of expanded subclones (suggestive of homogenizing selection events occurring in three separate GCs), one of which included the known high-affinity light chain mutation in position 119 (Fig. 5 g). Thus, *IgH^{CGG/+}* B cells are capable of SHM and antigen-driven selection to an extent similar to that of WT B cells bearing the same Ig rearrangements.

Discussion

We report the development of a hybrid method for the generation of B cell monoclonal mice that occupies an intermediate position between randomly inserted Ig transgenes and full two-chain Ig knock-ins. As with randomly inserted transgenes, our monoallelic Ig mice can be generated within 2–3 mo and do not require the transmission of two alleles, greatly expediting mouse generation and subsequent breeding to other genetically modified strains. Another potential advantage of this method is that because heavy and light chain sequences are paired at the mRNA level, paired heavy and light chain SHM analysis is possible using standard bulk deep sequencing, without the need for single-cell sorting or droplet-based approaches (Georgiou et al.,

2014; DeKosky et al., 2015), which may be advantageous under certain conditions.

Potential caveats of our approach include the lower expression of sIg (although we could not rule out that the lower expression of IgM and IgD is not a feature of this particular anti-GCC BCR), the apparently lower-than-normal rate of on-target hypermutation of V regions, and the residual off-target hypermutation of Cκ and the P2A peptide, all of which may alter the progression of the GC reaction. Notwithstanding, CSR and affinity-based selection—arguably the key reasons to use mice with Ig knock-in alleles rather than randomly inserted Ig transgenes—appear to be largely preserved, as determined by the ability of our knock-in strain to class switch both in vitro and in vivo and to accumulate mutations similar to those detected in two instances of natural evolution of that particular CGG-reactive clone (Tas et al., 2016). We therefore expect that monoallelic Ig knock-in mice could greatly facilitate the study of hypermutation and affinity maturation trajectories of monoclonal B cells. This would be especially useful for studies that require generation of a large panel of monoclonal mice, such as investigations of the origin and evolution of broadly neutralizing antibodies in HIV (Dosenovic et al., 2015) or of pathogenic autoantibodies in autoimmune disease (Degn et al., 2017).

Materials and methods

Design and cloning of the targeting construct

To generate the targeting construct, we first synthesized a shuttle vector containing an ~500-bp IgH-V promoter, a V_H leader sequence followed by an XhoI site, a human Cκ chain and the P2A peptide (both recoded to eliminate AID hotspots), a second

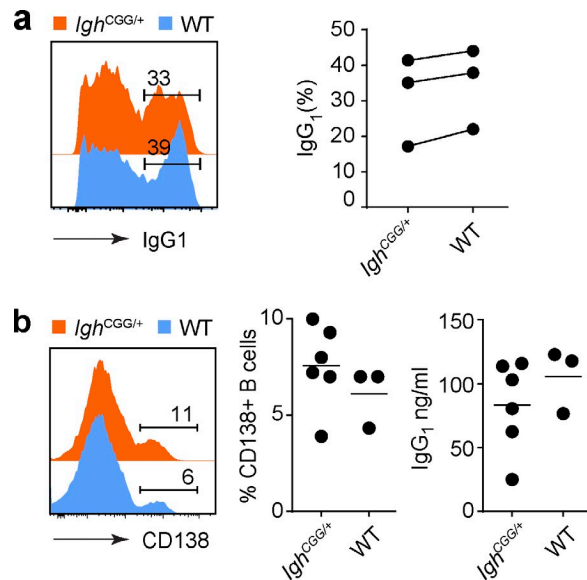


Figure 5. Isotype switching and plasmablast differentiation in *IgH^{CGG/+}* mice in vitro. (a) In vitro isotype switching. Purified *IgH^{CGG/+}* (CD45.2/2) and WT (CD45.1/1) B cells were cocultured in vitro with LPS and IL-4 to induce isotype switching to IgG₁. Histogram shows IgG₁ staining by flow cytometry on day 3 of culture. Data are from three independent experiments and are quantified in the graph; proportions of IgG₁⁺ cells in *IgH^{CGG/+}* and WT B cells from the same experiment are connected by a line. $P = 0.74$ (unpaired *t* test). (b) AFC cell formation (as defined by CD138 expression) and IgG₁ secretion in purified B cells stimulated with LPS and IL-4 in vitro. Cells were presorted as in Fig. 3a, and non-CGG-binding B cells were excluded from *IgH^{CGG/+}* cultures. Histograms are representative of, and graphs show pooled data for two independent experiments. $n = 3$ mice for WT and $n = 6$ mice for *IgH^{CGG/+}* CGG binding B cells. $P = 0.33$ for CD138 expression and $P = 0.37$ for supernatant IgG₁. Numbers within flow plots indicate percentage of cells in the designated gate.

V_H leader sequence followed by an AflII site, and part of the J_H4 intron including 50 bp starting from the splice donor (Fig. S1). To avoid repetitive sequences that would prevent gene synthesis, one of the V_H leaders was recoded. This fragment was cloned into Zero Topo blunt (451245; Thermo Fisher). Subsequently, the VJ_κ of the anti-CGG antibody (Tas et al., 2016) was cloned into the XhoI site and the VD_{JH} of the same antibody was cloned into the AflII site. This full construct was cloned into a previously designed vector containing 3' and 5' homology arms for insertion into the IgH locus (Sonoda et al., 1997). As the original vector with the IgH locus homology arms (Sonoda et al., 1997) was used for generating embryonic stem cell lines with IgH insertions, it contained a diphtheria toxin A selection cassette, which we removed by subcloning the full targeting insert (5' homology arm-Ig transgene-3' homology arm) into pBluescript KS. For injection, the final plasmid was purified using an endotoxin-free maxiprep kit (12362; QIAGEN).

sgRNA generation

To make each sgRNA, a gBlock with a built-in T7 priming sequence and the guide/scaffold sequence was synthesized using the sequence 5'-CGCTGTTAATACGACTCACTATAGGG_{n(20)}GTTT TAGAGCTAGAAATAGCAAGTTAAAATAAGGCTAGTCCGTTA TCAACTTGAAAAAGTGGCACCGAGTCGGTGCTTTT-3', where *n*₍₂₀₎ represents the location of the 20-bp CRISPR RNA sequence.

The lyophilized gblock was reconstituted in 10 μl of PCR-grade water to make 20 ng/μl stock. RNA was synthesized in vitro from the gblock using MEGAscript T7 kit (AM1354M; LifeTech) using 8 μl of the reconstituted gblock as a template. To clean up the RNA for synthesis, we used Agencourt RNAClean XP beads (A63987). We added 50 μl of beads for the synthesized RNA and incubated for 10 min. Using a 95-W plate magnet, the beads were washed three times in 80% EtOH. After the final EtOH wash, beads were briefly left to dry and resuspended in HyClone Molecular Biology-Grade Water (SH30538.02; GE Healthcare Life Sciences). Beads were removed from the solution after a 5-min incubation. The RNA was stored at -80°C until use. After testing, the superior guide sequences (*n*₍₂₀₎; see above) were determined to be 5'-GGAGCCGGCTGAGAGAAGTT-3' for 3' homology arm proximal targeting and 5'-CAGGGGCAGCCTGAGCTATG-3' for 5' homology arm proximal targeting.

Testing sgRNA cutting efficiency in blastocysts

To test the efficiency of our sgRNAs, they were injected individually into blastocysts (as detailed below). Blastocysts were cultured until E4.5 and collected into tubes with 5 μl QuickExtract buffer (QE09050; Epicentre). To obtain PCR-ready genomic DNA, we incubated the tubes at 65°C for 6 min, followed by a quick vortex and a 2 min incubation at 98°C. The entire 5 μl was used as a PCR template. For the 1-kb sequence spanning the 5' cutting site we used the following primers: forward 5'-AGAGATACTGCTTCA TCACA-3' and reverse 5'-GGGACCTGCACCTATCCTGTCC-3'. For the 1 kb sequence spanning the 3' cut site, we used the following primers: forward, 5'-ATAGGTTATGAGAGAGCCTCAC-3' and reverse 5'-CTGACAGTTGATGGTGACAATT-3'. We performed a PCR with Taq polymerase (M0273; New England Biolabs) at 95°C for 30 s, 30 cycles of 95°C for 30 s, 58°C for 60 s, and 68°C for 30 s, and a final extension time of 68°C for 5 min. PCR products were Sanger sequenced using their respective forward primers.

Zygote injections

Zygote injections were performed at the Genetically Engineered Models Center of the Whitehead Institute for Biomedical Research. All procedures were performed according to National Institutes of Health guidelines and approved by the Committee on Animal Care at Massachusetts Institute of Technology. Superovulated 8–10-wk-old female B6D2F2 mice (7.5 IU of pregnant mare serum gonadotropin [367222-1000IU; EMD Millipore], followed 46–48 h later by 7.5 IU chorionic gonadotropin [80051-032; VWR]) were mated to stud males, and fertilized pronuclear stage embryos (zygotes) were collected ~20 h after injection of human chorionic gonadotropin. Cytoplasmic injections were performed using a Piezo actuator (PMM-150FU; Prime Tech) and a flat-tip microinjection pipette with an internal diameter of 8 μm (Origio). The injection mix was prepared immediately before the procedure and included the following components at the final concentrations indicated: 100 ng/μl Cas9 mRNA (CAS9MRNA-1EA; Sigma Aldrich), 50 ng/μl sgRNA, 200 ng/μl of our IgH-targeting plasmid, and 1 mM SCR-7 (M60082-2s; Excess Biosciences) that inhibits non-homologous end joining (Maruyama et al., 2015) following the procedure published previously (Yang et al., 2014). Immediately after the completion of

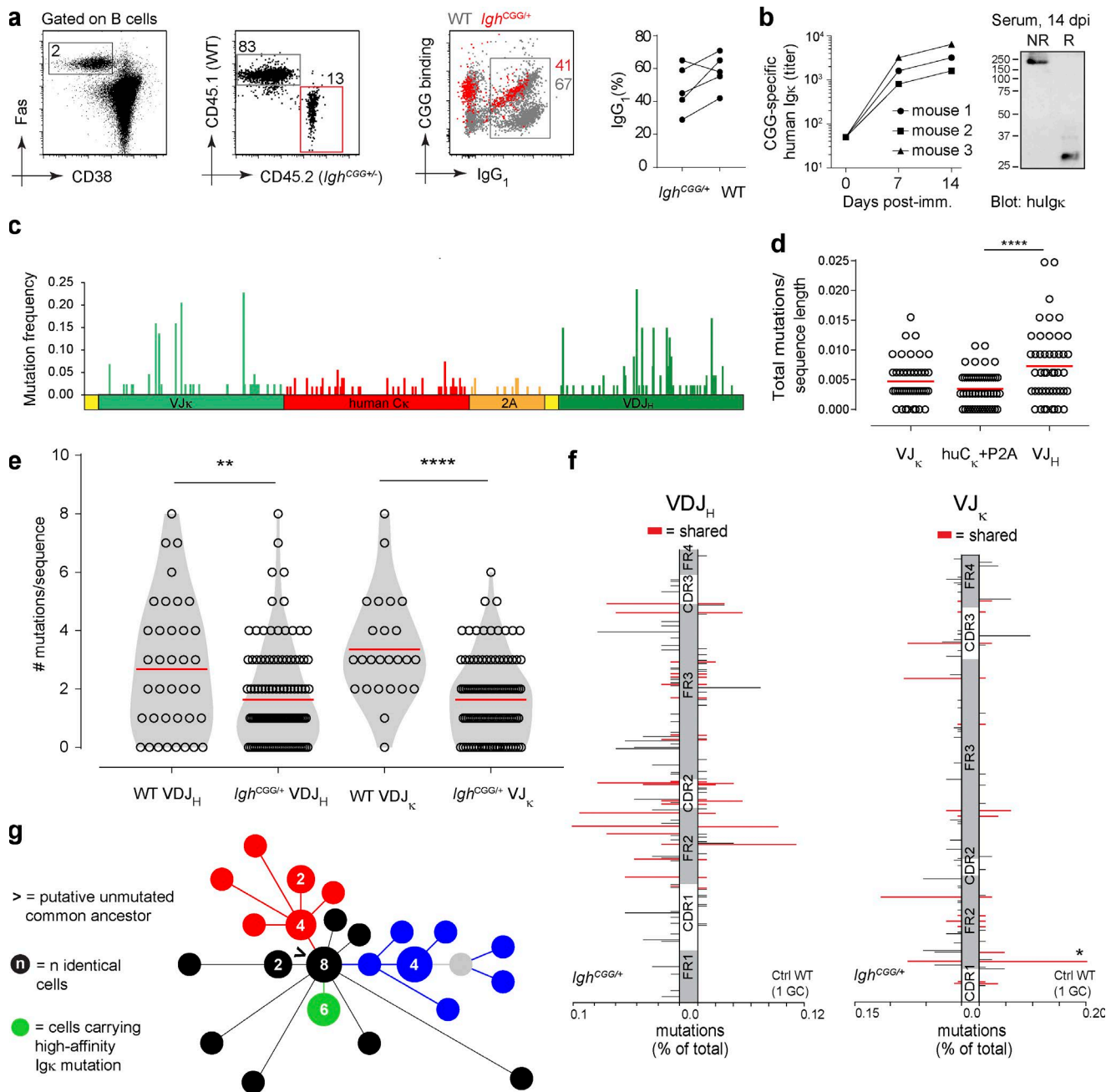


Figure 6. CSR, SHM, and antigen-driven selection in *IgH^{CGG/+}* B cells. (a) *IgH^{CGG/+}* B cells (CD45.2/2) were adoptively transferred into WT (CD45.1/1) recipients, which were immunized 1 d later with CGG in alum. CSR to IgG₁ was determined in GC B cells (CD19⁺TCRβ⁺Fas⁺CD38^{lo}) from donor (CD45.2/2) and recipient (CD45.1/1) mice by flow cytometry. Graph shows percentage of IgG₁⁺ GC B cells in five mice from two independent experiments. Proportions of switched cells in the same mouse are connected by a line. $P = 0.23$ (unpaired *t* test). Numbers within flow plots indicate percentage of cells in the designated gate. (b) Left: Serum titer of IgG₁⁺/human Cκ⁺ Ig in three mice adoptively transferred with *IgH^{CGG/+}* B cells and immunized with CGG. Graph shows data for three mice from two independent experiments. Right: Western blot for human Igκ in serum of mice adoptively transferred with *IgH^{CGG/+}* B cells and immunized with CGG 14 d after immunization. NR, nonreducing conditions; R, reducing conditions (DTT). Blot is representative of two experiments. (c–f) GC B cells from adoptive transfer experiments as in panel a were single sorted, and the entire *IgH^{CGG/+}* allele was PCR-amplified and sequenced. (c) Nucleotide mutation frequencies along the *IgH^{CGG/+}* locus, calculated as the fraction of times a particular nucleotide was mutated from the original sequence. (d) Total mutation frequency per region (normalized to sequence length). Each symbol represents one cell. (e) Number of nucleotide mutations in VDJ_H and VJ_K in *IgH^{CGG/+}* GC B cells compared with WT GC B cells carrying the same rearrangement selected by CGG immunization, as reported previously (Tas et al., 2016; only data from LN#2 GC2 in Fig. 4 from Tas et al., 2016 are analyzed). Data from two transfers of *IgH^{CGG/+}* B cells are pooled and compared with the WT. **, $P \leq 0.001$; ****, $P \leq 0.0001$ (unpaired *t* test). (f) Comparison of nucleotide mutation patterns between *IgH^{CGG/+}* B cells and WT GC B cells carrying the same rearrangement. Mutation patterns are shown for FR1 to FR4 regions of IgH and CDR1 to FR4 regions of Igκ. Shared nucleotide mutation positions are shown in red. Asterisk indicates a C119>G mutation, which confers an approximately eightfold gain in affinity. Data from two transfers of *IgH^{CGG/+}* B cells are pooled and compared with the WT. (g) Reconstructed phylogeny of *IgH^{CGG/+}* GC B cell VJ Igκ sequences from multiple GCs in one LN. Clades of expanded clones are indicated in red, green, and blue. Cells containing the high-affinity C119>G mutation are indicated in green.

the injection, ~20 zygotes were transferred into the oviducts of pseudopregnant ICR females (CD-1; Charles River) at 0.5 dpc. All protocols were approved by the Institutional Animal Care and Use Committee of the Massachusetts Institute of Technology.

Recombinant antibody production

293F cells were cotransfected with anti-CGG VDJ heavy chain (Tas et al., 2016) and anti CGG VJ WT (Tas et al., 2016) or IgK-2A light chain plasmids (see sequence data in Fig. S2) containing human constant regions, as described previously (Pasqual et al., 2015). mAbs were purified using protein G sepharose 4 Fast Flow resin (17061801; GE Healthcare Life Sciences) and dialyzed into PBS after elution. Concentrations were measured using a Thermo Fisher Scientific NanoDrop spectrophotometer.

Western blotting

B cells were purified from spleen with Miltenyi CD45R isolation beads (130-049-501; Miltenyi) with 0.5×10^6 cells used for every well. The cells were incubated in RIPA buffer for 2 min at room temperature. Loading buffer (NP0007; Invitrogen) and sample buffer (NP0009; Invitrogen) was added to the samples. The cell lysis samples (Fig. 2 d) were sonicated for 5 min, spun down for 2 min, and incubated at 90°C for 5 min. The serum samples (Fig. 6 a) were diluted in sample buffer and loaded on an SDS-PAGE gel. To reduce disulfide bonds, one sample was incubated for 10 min with DTT before loading. The samples were run on a 4–12% bis-tris NuPage gel (NP0322; Thermo Fisher) with 7 μ l prestained SeeBlue Plus2 (LC5925; Invitrogen). The gel was run in MOPS running buffer at 120 V for 1.5 h and then blotted onto a polyvinylidene difluoride membrane (Millipore Immobilon polyvinylidene difluoride membrane IPVH20200) in transfer buffer at 4°C for 1 h at 300 mA. After transfer, the membrane was incubated in blocking buffer at room temperature for 2 h. Goat anti-mouse IgM (1:6,000; Gerald et al., 2007) or goat anti-human C κ HRP (AP502P, 1:2,000; Millipore Sigma) was added to the blocking buffer and incubated for 1 h at room temperature. The membrane was rinsed three times with PBS with 0.05% Tween20 (P9416; Millipore Sigma). After drying, membranes were developed with 5–6 ml of Hyglo Quick spray (E2400; Denville Scientific). Chemiluminescence was detected after a 30 s or 20 min incubation. For the loading controls, the membrane was stripped and restained with 1:15,000 anti- β actin (GTX109639; GeneTex).

Southern blotting

A Southern blot was performed as described previously (Shih et al., 2002). Genomic DNA was digested with EcoRV.

ELISAs

Antigen-specific ELISAs were performed by coating plates with 10 μ g/ml chicken IgY (IgY-100; Gallus Immunotech) and detected with anti-human IgG-HRP (2040-05; Southern Biotech) at 1:10,000 dilution (Fig. 2 b) or with goat anti-human C κ HRP (AP502P; Millipore Sigma; Fig. 6 b) at 1:4,000 dilution. Isotype-specific ELISAs were performed by coating with goat anti-mouse IgG₁ (1070-01; SouthernBiotech) at 1 μ g/ml and detecting with goat anti-mouse IgG₁ (1070-05; SouthernBiotech) at 1:5,000 dilution (Fig. 6 c). For determination of IgG₁ in culture

supernatant (Fig. 6 c), mouse IgG₁ (5300-01B; SouthernBiotech) was used as a standard.

Cell transfers and immunizations

Adoptive transfer of CGG-specific B cells was performed by transferring either blood (Fig. 2 c) or purified B cells (Fig. 2 b and Fig. 6, a and b) from donor to recipient. For B cells transferred in blood, 100 μ l of blood (corresponding to $\sim 4 \times 10^5$ B cells) was collected from a donor mouse and directly injected intravenously into the recipient. For transfer of purified B cells, we isolated B cells from total splenocyte preparations by negative selection using anti-CD43-coupled magnetic beads (130-090-862; Miltenyi Biotec). Untouched B cells were purified according to the manufacturer's protocol, and 5×10^5 B cells were transferred into each recipient. 24 h following cell transfers, mice were immunized in each footpad with 10 μ g CGG precipitated in 1/3 vol Imject Alum (77161; ThermoFisher Scientific; Fig. 5) or in each footpad and also intraperitoneally with CGG in 1/2 vol Addavax (vac-adx-10; InvivoGen; 10 μ g/footpad and 20 μ g intraperitoneally per mouse; Fig. 6, a and b). To distinguish our transferred B cells, we used CD45.1 congenic mice as recipients (strain 002014; Jackson Laboratories). All protocols were approved by the Institutional Animal Care and Use Committee of the Rockefeller University.

Sample processing for flow cytometry and cell sorting

LN samples were placed in microcentrifuge tubes containing 100 μ l of PBS supplemented with 0.5% BSA and 1 mM EDTA (PBE), macerated using disposable micropestles (AXY-PES-15-B-SI; Axygen), and further dissociated into single-cell suspensions by gentle vortexing. 100 μ l of 2 \times antibody stain (antibodies to CD38, IgD, FAS, B220, and CD4 supplemented with Fc block) was added to the cell suspension, which was incubated on ice for 30 min. Single cells were sorted into 96-well plates (as described below) or bulk sorted into 15-ml conical tubes using a FACS Aria II cell sorter.

Antibodies for flow cytometry analysis

See Table S1 for detailed information about antibodies used for phenotyping CGG B cell mice, adoptive transfer, and isotype-switching experiments.

Single-cell *Igh* and *Igk* PCR and sequence analysis

Sorted single cells processed and analyzed essentially as described previously (Tas et al., 2016). Single-cell variable regions were amplified by seminested PCR using 5'-ATGGGTTGGTCCTGCATTATA CTGT-3' (forward L-VH recoded) with 5'-GGAAGGTGTGCACAC CGCTGGAC-3' (reverse IgG₁) and 5'-AGGGGGCTCTCGCAGGAG ACGAGG-3' (reverse IgM) for the first PCR and forward and 5'-GCTCAGGGAAATARCCCTTGAC-3' (IgG₁ internal reverse) for the second PCR. PCRs were performed with Taq polymerase (MO273; NEB). Products were amplified with the following program 94°C for 2 min, 29 rounds of 94°C for 30 s, 56°C for 30 s and 72°C for 55 s, followed by a final extension of 72°C for 10 min. Products were sent for sequencing with the primers 5'-GAATGTACACCGGTTGCAGTT GCTA-3' to obtain human C κ and 2A, 5'-ATGGGTTGGTCCTGCATT ATACTGT-3' to obtain VJ, and 5'-GCTCAGGGAAATARCCCTTGAC-3' (IgG₁ internal reverse) to obtain VDJ. Analysis of flow cytometry data for presentation was performed using FlowJo software v10.

Isotype-switching assay

In vitro isotype switching was essentially performed as previously described (Kracker and Radbruch, 2004). Untouched B cells were isolated using Miltenyi separation beads and columns and cultured at 3×10^5 cells/ml in 24-well tissue culture-coated plates. The cells were cultured in complete medium (RPMI-1640 medium plus glutamine; 10-040-CV; Corning cellgro) containing 100 U/ml penicillin and 100 µg/ml streptomycin (P11-010; PAA Laboratories), 10% FCS (heat inactivated, SH30910.03; GE Healthcare Life Sciences), and 5×10^{-5} M 2-mercaptoethanol (M7552; Sigma), 20 ng/ml recombinant IL-4 (574302, BioLegend), and 40 ng/ml LPS (*Escherichia coli* LPS serotype 055:B5 L2880; Sigma). The cells were stained for IgG₁ on day 4.

Statistical analysis

Differences in means for two-sample comparisons were evaluated using the two-tailed Student's *t* test.

Online supplemental material

Fig. S1 shows the sequence of the *Igh*^{CGG} insertion used to generate the monoclonal BCR mice described herein. Fig. S2 shows the sequence of the light chain plasmid used for recombinant antibody production. Table S1 lists the reagents used for flow cytometry.

Acknowledgments

We thank Yotam Bar On and the gene targeting resource center (The Rockefeller University) for technical advice and assistance.

This work was funded by National Institute of Allergy and Infectious Diseases (grants R01AI119006 and R21AI138020) and the Searle Scholars Program (G.D. Victora), the Research Council of Norway (program 239757), co-funded by the European Union's Seventh Framework Programme for research, technological development, and demonstration under Marie Curie grant agreement 608695 (J.T. Jacobsen), CAPES fellowship/PDSE/process number 88881.132337/2016-01 (C.B. Cavazzoni), and a Boehringer Ingelheim Fonds fellowship (A. Shiepers).

The authors declare no competing financial interests.

Author contributions: J.T. Jacobsen and G.D. Victora designed the study, targeting strategy (along with R. Jaenisch), and all experiments and wrote the manuscript. J.T. Jacobsen carried out all of the experimental work with assistance from L. Mesin, A. Schiepers, C.B. Cavazzoni, and D. Bousbaine. S. Markoulaki performed all zygote injections and wrote the related sections of the manuscript.

Submitted: 13 November 2017

Revised: 5 July 2018

Accepted: 16 August 2018

References

Benschop, R.J., K. Aviszus, X. Zhang, T. Manser, J.C. Cambier, and L.J. Wysocki. 2001. Activation and anergy in bone marrow B cells of a novel immunoglobulin transgenic mouse that is both hapten specific and autoreactive. *Immunity*. 14:33–43. [https://doi.org/10.1016/S1074-7613\(01\)00087-5](https://doi.org/10.1016/S1074-7613(01)00087-5)

Bloom, D.D., J.L. Davignon, P.L. Cohen, R.A. Eisenberg, and S.H. Clarke. 1993. Overlap of the anti-Sm and anti-DNA responses of MRL/Mp-lpr/lpr mice. *J. Immunol.* 150:1579–1590.

Casellas, R., T.A. Shih, M. Kleinewietfeld, J. Rakonjac, D. Nemazee, K. Rajewsky, and M.C. Nussenzweig. 2001. Contribution of receptor editing to the antibody repertoire. *Science*. 291:1541–1544. <https://doi.org/10.1126/science.1056600>

Chen, Y., J. Zhang, K.K. Hwang, H. Bouton-Verville, S.M. Xia, A. Newman, Y.B. Ouyang, B.F. Haynes, and L. Verkoczy. 2013. Common tolerance mechanisms, but distinct cross-reactivities associated with gp41 and lipids, limit production of HIV-1 broad neutralizing antibodies 2F5 and 4E10. *J. Immunol.* 191:1260–1275. <https://doi.org/10.4049/jimmunol.1300770>

Degn, S.E., C.E. van der Poel, D.J. Firl, B. Ayoglu, F.A. Al Qureshah, G. Bajic, L. Mesin, C.A. Reynaud, J.C. Weill, P.J. Utz, et al. 2017. Clonal Evolution of Autoreactive Germinal Centers. *Cell*. 170:913–926.e19.

DeKosky, B.J., T. Kojima, A. Rodin, W. Charab, G.C. Ippolito, A.D. Ellington, and G. Georgiou. 2015. In-depth determination and analysis of the human paired heavy- and light-chain antibody repertoire. *Nat. Med.* 21:86–91. <https://doi.org/10.1038/nm.3743>

Dosenovic, P., L. von Boehmer, A. Escolano, J. Jardine, N.T. Freund, A.D. Gitlin, A.T. McGuire, D.W. Kulp, T. Oliveira, L. Scharf, et al. 2015. Immunization for HIV-1 Broadly Neutralizing Antibodies in Human Ig Knockin Mice. *Cell*. 161:1505–1515. <https://doi.org/10.1016/j.cell.2015.06.003>

Escolano, A., J.M. Steichen, P. Dosenovic, D.W. Kulp, J. Golijanin, D. Sok, N.T. Freund, A.D. Gitlin, T. Oliveira, T. Araki, et al. 2016. Sequential Immunization Elicits Broadly Neutralizing Anti-HIV-1 Antibodies in Ig Knockin Mice. *Cell*. 166:1445–1458.e12.

Ewulonu, U.K., L.J. Nell, and J.W. Thomas. 1990. VH and VL gene usage by murine IgG antibodies that bind autologous insulin. *J. Immunol.* 144:3091–3098.

Georgiou, G., G.C. Ippolito, J. Beausang, C.E. Busse, H. Wardemann, and S.R. Quake. 2014. The promise and challenge of high-throughput sequencing of the antibody repertoire. *Nat. Biotechnol.* 32:158–168. <https://doi.org/10.1038/nbt.2782>

Geraldes, P., M. Rebrovich, K. Herrmann, J. Wong, H.M. Jäck, M. Wabl, and M. Cascalho. 2007. Ig heavy chain promotes mature B cell survival in the absence of light chain. *J. Immunol.* 179:1659–1668. <https://doi.org/10.4049/jimmunol.179.3.1659>

Goodnow, C.C., J. Crosbie, S. Adelstein, T.B. Lavoie, S.J. Smith-Gill, R.A. Brink, H. Pritchard-Briscoe, J.S. Wotherspoon, R.H. Loblay, K. Raphael, et al. 1988. Altered immunoglobulin expression and functional silencing of self-reactive B lymphocytes in transgenic mice. *Nature*. 334:676–682. <https://doi.org/10.1038/334676a0>

Goodnow, C.C., J. Crosbie, H. Jorgensen, R.A. Brink, and A. Basten. 1989. Induction of self-tolerance in mature peripheral B lymphocytes. *Nature*. 342:385–391. <https://doi.org/10.1038/342385a0>

Kracker, S., and A. Radbruch. 2004. Immunoglobulin class switching: in vitro induction and analysis. *Methods Mol. Biol.* 271:149–159.

Lam, K.P., and K. Rajewsky. 1999. B cell antigen receptor specificity and surface density together determine B-1 versus B-2 cell development. *J. Exp. Med.* 190:471–477. <https://doi.org/10.1084/jem.190.4.471>

Manz, J., K. Denis, O. Witte, R. Brinster, and U. Storb. 1988. Feedback inhibition of immunoglobulin gene rearrangement by membrane mu, but not by secreted mu heavy chains. *J. Exp. Med.* 168:1363–1381. <https://doi.org/10.1084/jem.168.4.1363>

Maruyama, T., S.K. Dougan, M.C. Truttmann, A.M. Bilate, J.R. Ingram, and H.L. Ploegh. 2015. Increasing the efficiency of precise genome editing with CRISPR-Cas9 by inhibition of nonhomologous end joining. *Nat. Biotechnol.* 33:538–542. <https://doi.org/10.1038/nbt.3190>

Mason, D.Y., M. Jones, and C.C. Goodnow. 1992. Development and follicular localization of tolerant B lymphocytes in lysozyme/anti-lysozyme IgM/IgD transgenic mice. *Int. Immunol.* 4:163–175. <https://doi.org/10.1093/intimm/4.2.163>

Nussenzweig, M.C., A.C. Shaw, E. Sinn, D.B. Danner, K.L. Holmes, H.C. Morse III, and P. Leder. 1987. Allelic exclusion in transgenic mice that express the membrane form of immunoglobulin mu. *Science*. 236:816–819. <https://doi.org/10.1126/science.3107126>

Pasqual, G., A. Angelini, and G.D. Victora. 2015. Triggering positive selection of germinal center B cells by antigen targeting to DEC-205. *Methods Mol. Biol.* 1291:125–134. https://doi.org/10.1007/978-1-4939-2498-1_10

Pelanda, R., S. Schaal, R.M. Torres, and K. Rajewsky. 1996. A prematurely expressed Ig(kappa) transgene, but not V(kappa)J(kappa) gene segment targeted into the Ig(kappa) locus, can rescue B cell development in lambda5-deficient mice. *Immunity*. 5:229–239. [https://doi.org/10.1016/S1074-7613\(00\)80318-0](https://doi.org/10.1016/S1074-7613(00)80318-0)

- Rusconi, S., and G. Köhler. 1985. Transmission and expression of a specific pair of rearranged immunoglobulin mu and kappa genes in a transgenic mouse line. *Nature*. 314:330–334. <https://doi.org/10.1038/314330a0>
- Sakurai, T., S. Watanabe, A. Kamiyoshi, M. Sato, and T. Shindo. 2014. A single blastocyst assay optimized for detecting CRISPR/Cas9 system-induced indel mutations in mice. *BMC Biotechnol.* 14:69. <https://doi.org/10.1186/1472-6750-14-69>
- Shih, T.A., M. Roederer, and M.C. Nussenzweig. 2002. Role of antigen receptor affinity in T cell-independent antibody responses in vivo. *Nat. Immunol.* 3:399–406. <https://doi.org/10.1038/ni776>
- Sonoda, E., Y. Pewzner-Jung, S. Schwers, S. Taki, S. Jung, D. Eilat, and K. Rajewsky. 1997. B cell development under the condition of allelic inclusion. *Immunity*. 6:225–233. [https://doi.org/10.1016/S1074-7613\(00\)80325-8](https://doi.org/10.1016/S1074-7613(00)80325-8)
- Sweet, R.A., S.R. Christensen, M.L. Harris, J. Shupe, J.L. Sutherland, and M.J. Shlomchik. 2010. A new site-directed transgenic rheumatoid factor mouse model demonstrates extrafollicular class switch and plasmablast formation. *Autoimmunity*. 43:607–618. <https://doi.org/10.3109/08916930903567500>
- Taki, S., M. Meiering, and K. Rajewsky. 1993. Targeted insertion of a variable region gene into the immunoglobulin heavy chain locus. *Science*. 262:1268–1271. <https://doi.org/10.1126/science.8235657>
- Tas, J.M., L. Mesin, G. Pasqual, S. Targ, J.T. Jacobsen, Y.M. Mano, C.S. Chen, J.C. Weill, C.A. Reynaud, E.P. Browne, et al. 2016. Visualizing antibody affinity maturation in germinal centers. *Science*. 351:1048–1054. <https://doi.org/10.1126/science.aad3439>
- Weaver, D., F. Costantini, T. Imanishi-Kari, and D. Baltimore. 1985. A transgenic immunoglobulin mu gene prevents rearrangement of endogenous genes. *Cell*. 42:117–127. [https://doi.org/10.1016/S0092-8674\(85\)80107-0](https://doi.org/10.1016/S0092-8674(85)80107-0)
- Yang, H., H. Wang, C.S. Shivalila, A.W. Cheng, L. Shi, and R. Jaenisch. 2013. One-step generation of mice carrying reporter and conditional alleles by CRISPR/Cas-mediated genome engineering. *Cell*. 154:1370–1379. <https://doi.org/10.1016/j.cell.2013.08.022>
- Yang, H., H. Wang, and R. Jaenisch. 2014. Generating genetically modified mice using CRISPR/Cas-mediated genome engineering. *Nat. Protoc.* 9:1956–1968. <https://doi.org/10.1038/nprot.2014.134>
- Yu, K., F.T. Huang, and M.R. Lieber. 2004. DNA substrate length and surrounding sequence affect the activation-induced deaminase activity at cytidine. *J. Biol. Chem.* 279:6496–6500. <https://doi.org/10.1074/jbc.M311616200>